Design of delay elements in a binary optical true-time-delay device that uses a White cell

S. Kunathikom, B. L. Anderson, and S. A. Collins, Jr.

A White-cell–based binary optical true-time-delay device has two parts: the controller, or switching engine, and the delay elements. Here we discuss in detail the design of both glass blocks and lens trains as delay elements. Glass blocks can be used in our design for delays ranging from one to a few hundred picoseconds. Lens trains are suitable for longer delays. We also analyze the loss associated with each design and give design limits. © 2003 Optical Society of America

OCIS codes: 280.5110, 070.1170, 200.4740, 230.3720.

1. Introduction

Optical devices that produce true-time delays for phased-array antennas have generated recent interest.[1] Published approaches include fiber delay lines,[2–5] wavelength division multiplexing,[6–8] Bragg gratings,[9–12] acousto-optics,[13] waveguides,[14,15] optoelectronic integrated circuits,[16] and free-space approaches.[17–20]

We have proposed an approach based on the White cell.[21–23] Briefly the original White cell[24] is an arrangement of mirrors that can provide multiple bounces for a large number of input beams, which are refocused on every bounce. Each beam forms a unique set of spots, with the number of spots being equal to the number of passes. A spatial light modulator (SLM) placed in the plane of the spots can thus switch each beam on each bounce. We switch among paths of varying lengths to produce the delays.

In this paper we are concerned with binary cells. These are devices that incorporate two White cells with a SLM to select between them. One switch state sends a beam to a null White cell path, whereas the other switch state sends the beam via another White cell to a delay element. It is possible for hundreds or thousands of light beams to circulate in the White cell simultaneously. Each input beam also makes a specific and unique spot pattern on the SLM. These spots are arranged in columns. In a binary cell we associate each column with a different delay; that is, on the first bounce, a beam sent to the delay element undergoes a time delay of Δ, where Δ is the time delay increment. On the second bounce the spot forms in the next column and the beam is delayed by 2Δ, and so on.

The binary cell has two main components: the switching engine, which contains the White cell and switches beams on each bounce to either the null path or a delay path, and the delay elements themselves. We have reported the switching engine separately.[25] Here we address in detail the design of the delay elements themselves. We organize the paper as follows. In Section 2 we briefly present the binary architecture and then discuss the use of glass blocks as delay elements. In Section 3 we address the problem of producing long delays while avoiding the divergence problem associated with all free-space approaches. In Section 4 we calculate the losses for each type of delay element. Finally, in Section 5 we provide a discussion and a summary.

2. The Binary Cell and Glass Blocks As Delay Elements

The top of Fig. 1 shows the original White cell,[24] which consists of three spherical mirrors: one field mirror (mirror A on the right) and two objective mirrors. A turning mirror is used to bring beams into and out of the cell. A beam bouncing back and forth between them is refocused to a spot on each pass. Because the White cell has been explained in detail elsewhere,[22,23,26] we will repeat only the main points

S. Kunathikom is with Schlumberger SCD, 555 Industrial Boulevard, Sugar Land, Texas 77478. B. L. Anderson (anderson@ee.eng.ohio-state.edu) and S. A. Collins, Jr. are with the Department of Electrical Engineering, Ohio State University, 205 Dreese Laboratory, 2015 Neil Avenue, Columbus, Ohio 43210.

Received 25 October 2002; revised manuscript received 5 September 2003.

0003-6935/03/356984-11$15.00/0

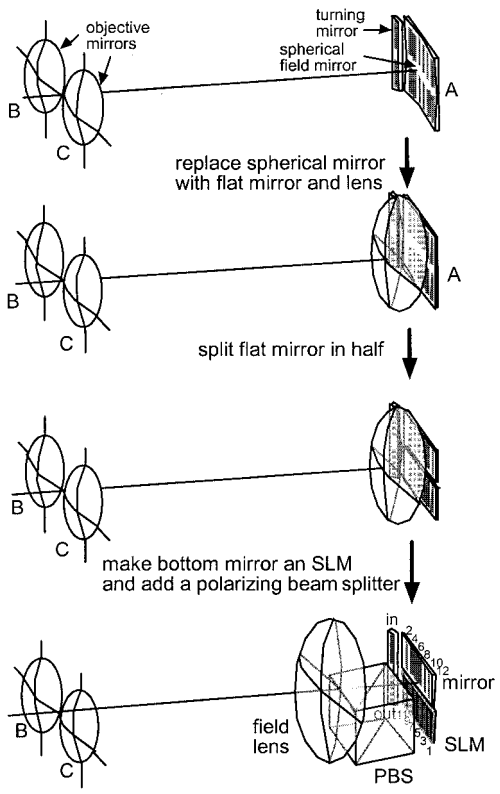

Fig. 1. In the original White cell (top), the field mirror, which is spherical, can be replaced with a flat mirror and a lens. The flat mirror can be divided into two parts, one for even-numbered light bounces and one for odd. Replacing one of these mirrors with a LC SLM (bottom) permits the beam to be switched on every bounce.

here. First, a beam circulating in the White cell traces out a particular spot pattern, usually in two rows, with, for example, even-numbered spots going from left to right across the top of the field mirror and odd-numbered spots going from right to left across the bottom. Second, many beams can simultaneously circulate inside the White cell. The figure shows a rectangular array of input spots that is reimaged multiple times on the field mirror. Each beam within that array, however, traces out a unique spot pattern that is independent of any other beam. In other words, none of the spots overlap or coincide.

Each of these spots represents an opportunity to switch a beam without affecting the others. To make it possible to switch beams as they travel back and forth, we replace field mirror A with a SLM. To make the transition from a simple White cell to a time-delay device, we first recognize that a spherical mirror is functionally the same as a flat mirror and a lens (second step in Fig. 1). Further, because the spots appear in two groups—even-numbered ones on top and odd-numbered ones on the bottom—we can divide the flat mirror into two mirrors that can then be separated in space. Then we let the bottom flat mirror be a SLM. Here we are assuming a liquid-crystal (LC) SLM; therefore, we add a polarizing beam splitter in front of it. We also move the field lens to the other side of the beam splitter.

Figure 2(a) shows that a second White cell can now be added. A beam whose polarization is horizontal passes through the beam splitter, and, provided its polarization remains the same, that beam circulates in the BC White cell. The beam makes its even-numbered bounces on the flat mirror labeled auxiliary mirror I and its odd numbered bounces on the SLM. If, however, on a particular bounce the polarization is changed by the SLM, then the beam is diverted by the beam splitter, and the light goes to the EF White cell. In this case, the light goes to mirror E, which forms the next even-numbered spot on auxiliary mirror II, and returns by mirror F and the beam splitter back to the SLM for the next odd-numbered spot.

Hundreds or thousands of beams can circulate simultaneously in the White cell. For simplicity, however, Figure 2(b) shows the spot pattern for only five hypothetical beams. They enter the White cell by means of the turning mirror on the left of the SLM plane, where they are imaged as spots. The turning mirror then directs the beams to mirror B, which reimages them onto an array of five new spots (bounce labeled 1) on the SLM. At this point each of the five spots lands on a different pixel, where its polarization can either be changed or remain the same. Each beam in this example makes 16 bounces in the White cell and can be switched to either auxiliary mirror I or II for its next even-numbered bounce.

To change this arrangement to a time-delay device, we replace auxiliary mirror II with some type of delay element. We choose here a set of glass (or other dielectric) blocks, as shown in Fig. 2(c). These blocks have a refractive index higher than that of air and thus slow the beams down. The back of each block is reflective, and it is here that the beams form their even-numbered spots. The beams return to the SLM in exactly the same place as if they had gone to auxiliary mirror I. This is because the centers of curvature of mirrors E and F are coaligned with the centers of curvature of mirrors B and C, respectively.[21] The beams that are sent to the glass blocks, however, are delayed compared with the beams sent to auxiliary mirror I. We will show that staggering the backs of the blocks and extending their fronts beyond the plane of the original auxiliary mirror II will preserve the imaging conditions of the White cell.

The first glass block produces a time delay of the chosen time increment Δ. A beam directed to the delay element on the second bounce takes Δ longer to return to the SLM than does a beam sent to auxiliary mirror I. The second glass block is twice as deep and produces a delay of 2Δ. The other blocks (4, 6, 8, etc.) delay the beam by 4Δ, 8Δ, 16Δ, and so forth. A beam sent to the delay element on every bounce accumulates the maximum relative time delay. If the total number of bounces is m, then there are $m/2$

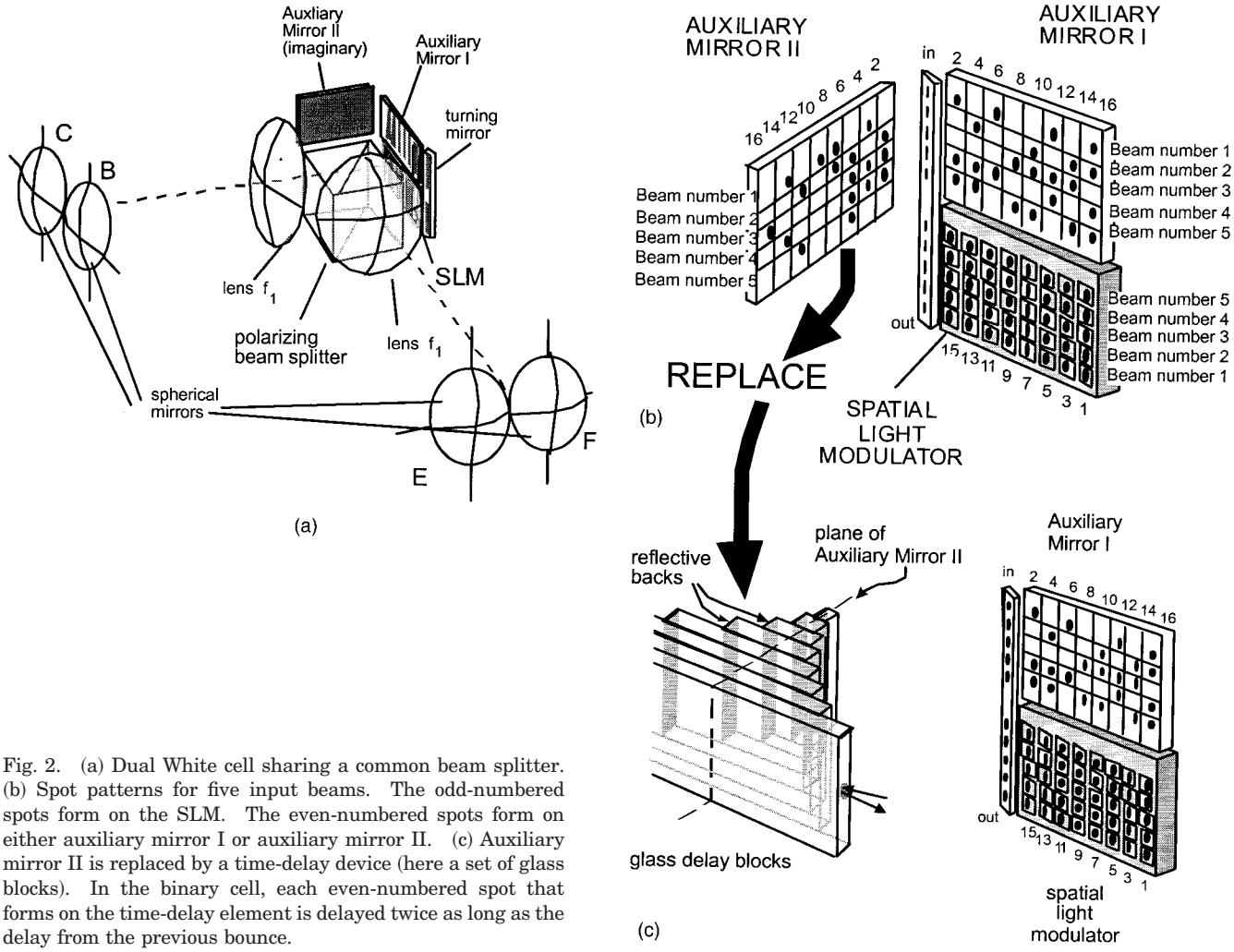

Fig. 2. (a) Dual White cell sharing a common beam splitter. (b) Spot patterns for five input beams. The odd-numbered spots form on the SLM. The even-numbered spots form on either auxiliary mirror I or auxiliary mirror II. (c) Auxiliary mirror II is replaced by a time-delay device (here a set of glass blocks). In the binary cell, each even-numbered spot that forms on the time-delay element is delayed twice as long as the delay from the previous bounce.

delay blocks, and the maximum delay N that can be produced is

$$N = 2^{m/2}. \quad (1)$$

We call this arrangement a binary cell. Any integer multiple of the time-delay increment Δ (from zero to N) can be obtained independently for each beam.

The number of bounces is fixed for all light beams; only the path changes. Note that a beam circulating entirely in the BC cell still incurs some overall delay. The propagation time of every beam through the White cell is at least as long as the overall delay. Because this delay is common to all beams, it is in effect subtracted out. It is the differences in the path lengths that create the relative delays.

A. Glass Block Design

To design a glass block to produce a delay of specified length, we must satisfy the imaging conditions of the White cell. In the original White cell, there are two imaging conditions: (1) either objective mirror must image the field mirror back onto itself and (2) The field mirror images one objective mirror onto the other. In the true-time-delay device, these conditions can be restated as follows:

1. The SLM must image onto auxiliary mirror 1 through either mirror B or C. Similarly the SLM must image onto the backs of the glass blocks through either mirror E or F.
2. Mirrors B and C must be imaged onto each other by either auxiliary mirror I and lens f_1 or the SLM and lens f_1; and mirrors E and F must image onto each other by either the SLM and lens f_2 or by the glass blocks and lens f_2.

Figure 3 shows a top view of the SLM, the beam splitter, lens f_1, and the White cell mirrors E and F. Conjugate to the SLM is a glass block of thickness d_2' set a distance d_2'' from the lens. The plane of the imaginary auxiliary mirror II is closer to the beam splitter than is the SLM's reflective surface in order to compensate for the refractive index of the polarizing beam splitter. The size of the polarizing beam splitter (dashed square) is d_1 and its refractive index is n_1. The BC White cell is equivalent, with $d_{BC} = d_{EF}$, $f_1 = f_2$, and $d_2'' = d_2$ ($d_2' = 0$), where f_1 is the focal length of lens f_1, etc.

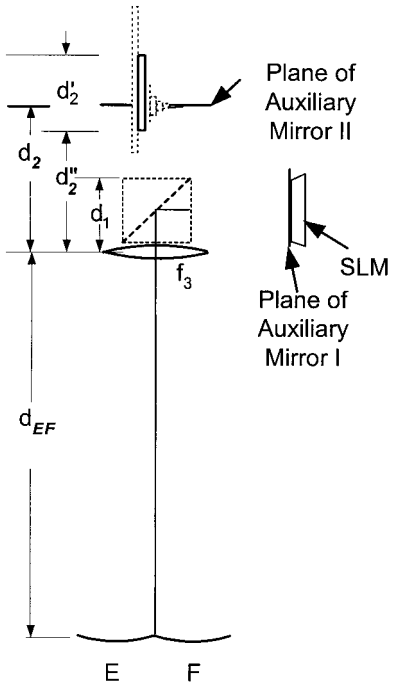

Fig. 3. Top view of a White cell containing a glass block delay element.

We use paraxial ray analysis to design the cell. That is, we write the ABCD matrices for each of the optical elements and then multiply them together to get the resulting matrix for a given path. To have imaging, we set the B element of the result equal to zero. As has been described elsewhere,[21,23] the condition that the objective mirrors must image onto each other gives the result that d_{EF} should be equal to f_1.

The focal length of the spherical mirror is found from the other imaging condition, which stipulates that the SLM must image onto the back of the glass block. Let us suppose for a moment that there is no glass block; that is, the reflective surface is at the location of the original auxiliary mirror II. If we write out the *ABCD* matrices for each of the optical elements in the path from the SLM to the auxiliary mirror position and set the B element of the product to zero to give imaging, we obtain the following result:

$$B = 0 = 2\left(d_{EF} - \frac{d_1}{n_1}\right) - \frac{{d_{EF}}^2}{f_1}. \tag{2}$$

This gives an expression for f, the focal length of the spherical mirror:

$$f = \frac{d_{EF}}{2\left(1 - \dfrac{d_1}{n_1 d_{EF}}\right)}. \tag{3}$$

Next we observe that when there is no glass block, the spots image on the equivalent auxiliary mirror plane. As glass is added, the distance d_2 between the lens and the reflective surface will increase. Let $d_{2\,\min}$ be the minimum possible distance between the lens and the reflective surface, which occurs in the BC White cell and contains auxiliary mirror I. The expression for $d_{2\,\min}$ is given by[21]

$$d_{2\,\min} = 2d_{BC} - \frac{{d_{BC}}^2}{f_1} - \frac{d_1}{n_1}. \tag{4}$$

The minimum possible transit time for one round trip through the cell occurs for a beam going through the BC White cell:

$$\begin{aligned} T_{\min} &= \frac{2}{c}\left(n_1 d_1 + 2d_{BC} + d_{2\,\min}\right) \\ &= \frac{2}{c}\left[n_1 d_1 + 2d_{BC} + 2\left(2d_{BC} - \frac{{d_{BC}}^2}{f_1} - \frac{d_1}{n_1}\right)\right]. \end{aligned} \tag{5}$$

Now we wish to introduce a specified delay. We not only need to choose the length of the glass block so that the overall transit time for one round trip is greater than $T_{\min}$ by some increment Δ, we must also continue to satisfy the imaging conditions. We write the matrix for the system, this time including matrices for the distance d_2'', the block length d_2', and the block index n_2. Setting the resulting B element to zero gives the following equation[21]:

$$\frac{d_2'}{n_2} + d_2'' = 2d_{EF} - \frac{{d_{EF}}^2}{f} - \frac{d_1}{n_1}. \tag{6}$$

The transit time T_I for one pass from the SLM to the reflective surface of the delay block and back is

$$\frac{cT_I}{2} = n_1 d_1 + 2d_{EF} + n_2 d_2' + d_2''. \tag{7}$$

Setting the desired time-delay increment to $\Delta = T_I - T_{\min}$, the results are

$$d_2' = \frac{n_2}{({n_2}^2 - 1)}\frac{c}{2}(\Delta T), \tag{8}$$

$$d_2 = d_{2\,\min} + \frac{1}{(n_2 + 1)}\frac{c}{2}\Delta T = d_2' + d_2'', \tag{9}$$

$$d_2'' = d_2 - d_2' = d_{2\,\min} + \left[\frac{1}{n_2 + 1} - \frac{n_2}{{n_2}^2 - 1}\right]\frac{c}{2}\Delta T. \tag{10}$$

Equations (8) and (10) together give the length and position required for a particular delay block.

B. Beam Divergence and Maximum Block Length

There is a limit to the length that a glass block can have before the sides of the block truncate the diverging beams. In this section we address the question of the maximum delay that we can obtain with this method.

Figure 4 illustrates this problem. A beam focused to a spot on the back of the glass block will necessarily

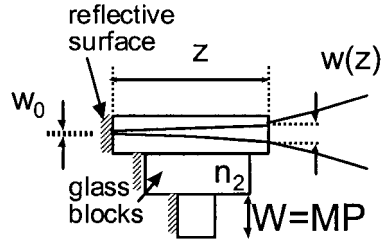

Fig. 4. There is a limit to the time delay that can be obtained with glass blocks because the beam divergence will eventually cause truncation.

diverge. The pixel pitch P on the SLM sets the width of the blocks because it is also the spot pitch. The spot size at the reflective back of the block is w_0, the beam waist. The spot size at the front of the block, for Gaussian beams, is given by

$$w(z) = w_0\left[1 + \left(\frac{2z}{n_2 k_0 {w_0}^2}\right)^2\right]^{1/2}, \tag{11}$$

where n_2 is the refractive index of the block; z is the length of the block; and $k_0 = 2\pi\ \lambda_0$, where λ_0 is the free-space wavelength. If we integrate the energy in the Gaussian spot of size $w(z)$ over a square region equal to the width of the block W, the resulting power ratio is

$$\frac{P_{\text{captured}}}{P_{\text{total}}} = \left\{\text{erf}\left[\frac{\sqrt{2}W}{2w(z)}\right]\right\}^2. \tag{12}$$

If we require that 99.99% of the energy be captured (not truncated), the result is that the spot size $w(z)$ (i.e., $1/e$ of the field) should be approximately equal to

$$\frac{w(z)}{W} \approx 0.26. \tag{13}$$

As an example, consider an LC SLM with 100-μm square pixels on a 250-μm pitch, and a light beam of $\lambda = 1.3$ μm. To maintain 99.99% of the energy when the beam reflects off the 100-μm pixel, the beam waist should be $w_0 = 26$ μm, from relation (13). If there is $M = 1$ magnification from the SLM to the glass blocks, then the block width is equal to the pixel pitch and $W = 250$ μm. Thus the beam of waist w_0 cannot expand to greater than a $1/\varepsilon$ field radius of $w(z) = 250\ \mu\text{m} \times 0.26 = 65\ \mu\text{m}$. Substituting into Eq. (11), we find the maximum block length of 3.0 mm for $n_2 = 1.5$, or an attainable round-trip delay of 30 ps.

There are two ways to improve this to achieve a little more range. One is to magnify the image of the SLM onto the plane of the glass blocks, thereby effectively increasing both the pitch and the tolerable block depth. This also has the effect of increasing the spot's size and thus reducing the beam divergence. The other way to increase the delays is to increase the refractive index of the delay blocks. Figure 5 shows the effects of both magnification and refractive index. Here we have plotted the maximum attainable delay for $\lambda = 1.3$ μm, $P = 250$ μm, and $w_0 = 26$ μm as a function of refractive index for various values of magnification. One can obtain delays into the nanosecond range by increasing both the refractive index and the magnification. The tradeoffs are that higher-index materials may be more expensive, and that increasing the magnification tends to increase the overall size of the apparatus.

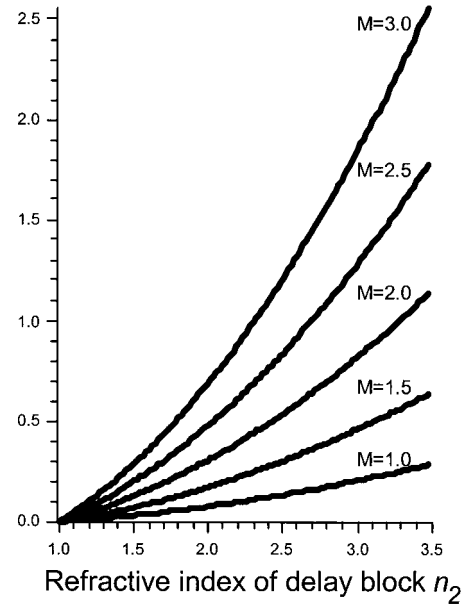

Fig. 5. Effect of magnification and refractive index on the maximum allowable delay for a glass block.

C. Glass Block Design Example

Let us now give a specific design example. We assume a wavelength of $\lambda = 1.3$ μm. The SLM is taken to be a 16×16 array of 100-μm square pixels on a 250-μm pitch. The beam waist is 25 μm, and the magnification of the SLM onto the glass blocks is taken to be $M = 1.67$, resulting in a block pitch of $W = 417.5$ μm. We take our basic time-delay increment to be 1 ps. Finally, we assume $n_2 = 1.5$.

Figure 6 shows a top view of the glass block assembly. We have 7 bits of delay, or seven blocks. The dotted line shows the position of the original auxiliary mirror II equivalent plane, and the distances A_b,

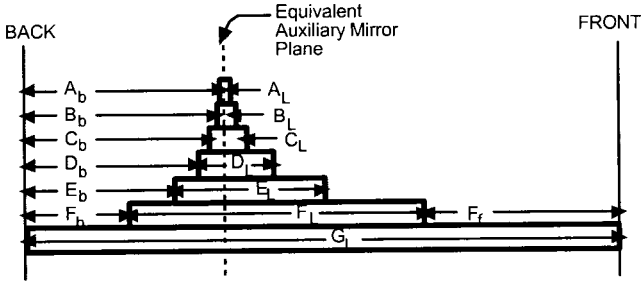

Fig. 6. Glass block design sample, with a time-delay increment of 1 ps. The dimensions are listed in Table 1.

Table 1. Dimensions for Glass Blocks of Design Sample

Dimension	Glass Block A	B	C	D	E	F	G
Time delay (ps)	1	2	4	8	16	32	64
Back distance of A_b, etc. (mm)	3.78	3.72	3.6	3.66	2.88	1.92	0
Length of A_L, etc. (mm)	0.18	0.36	0.72	1.44	2.88	5.76	11.52
Front distance of A_f, etc. (mm)	7.56	7.44	7.20	6.42	5.76	3.84	0

B_b, etc. are the distances from the back edge of the block assembly (the back of the longest block) to the backs of the individual blocks. The lengths are A_L, B_L, etc., and the front distances are A_f, B_f, and so on. The values, along with the delays, are given in Table 1. The maximum delay is obtained by visiting the glass blocks on every bounce for a total of $T = 127\Delta$. Including zero, this represents 128 different sequential delays.

3. Lens Trains

In Section 2 we saw that glass blocks could be used for short delays, but we still need a solution for long delays. To address this we replace auxiliary mirror II from Fig. 2 with a lens train, as shown in Fig. 7(a).[21] The spots are formed in columns on the entrance to the lens train, which is located on the right-hand side of the figure. Each group of lenses reimages the spots onto the next conjugate plane (CP). At each CP there is a mirror strip that reflects the spots in that particular column back. The other spots continue deeper into the lens train. In Fig. 7(a) we show five columns, which represent the five possible bounces to this plane (ten bounces total). We also show several lens groups with three lenses each. The spots are reimaged from the entrance plane onto each of the conjugate planes CP_1, CP_2, CP_3, etc. The center lens of each lens group performs the imaging. The other lenses are field lenses and are discussed below. First, however, let us slowly go through the operation of the lens train.

The beams enter from the right-hand side as spots. Those that arrive on the first even-numbered bounce (bounce 2) pass through the right-most column of the entrance plane, and the spots are reimaged onto CP_1 with magnification $M = -1$. This puts the column corresponding to bounce 2 on the left-hand side of CP_2. Here, there is a strip mirror that reflects the spots back so that they are reimaged back onto the entrance–exit plane and then propagate back into the White cell. The spots returning to the White cell look identical in terms of size, divergence, shape, etc., to those that would have struck the auxiliary mirror, except they have been delayed by an extra time increment equal to the round-trip propagation time between the lens train entrance plane and CP_1. This propagation time is the delay increment Δ.

Spots sent to the lens train on bounce 4 pass through the second column of the entrance plane, and when they arrive at CP_1 they are also in the second column and thus miss the strip mirror. These beams continue on and are reimaged to the second column of CP_2, where there is a second strip mirror. The round-trip time through these two lens groups is set to 2Δ; that is, the second lens group is the same length as the first. The length of the third lens group is equal to twice the length of the previous groups combined, or 4Δ, and so on, to create the binary sequence.

We said before that the center lens in each lens group images one conjugate plane onto the next, as shown in Figure 7(b). The center lens in each group mimics the function of the spherical mirrors (objective mirrors) E or F (or B or C) because it in effect images one spot pattern to another, just as E images the SLM plane onto the entrance to the lens train. Next we discuss the lenses positioned on either side of the conjugate planes: field lenses. They perform

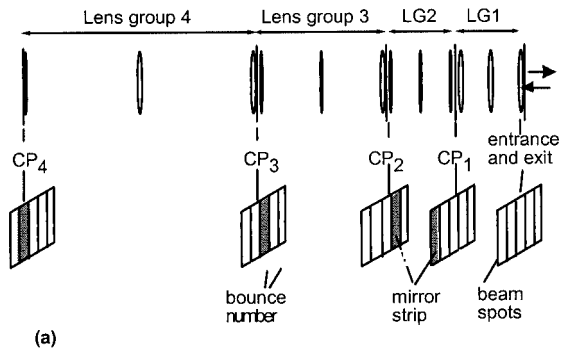

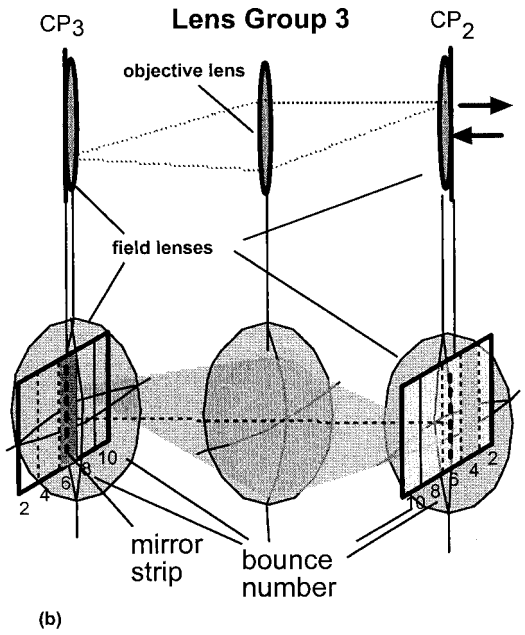

Fig. 7. Lens train (a) The spots are reimaged onto each conjugate plane. A mirror strip in each conjugate plane (CP) intercepts the appropriate column of the spot pattern and returns it to the White cell.[1] (b) Close-up of lens group 3.

the other imaging function of the White cell, which is equivalent to imaging one spherical mirror onto the other, such as E onto F.

For example, consider a beam entering the first lens group. Let us suppose that the beam in question is arriving during bounce 2, so that it will be reflected at CP_1. The lens at the right-hand side of lens group 1 images mirror E onto the center lens (White cell imaging condition 2). The center lens images the entrance plane onto CP_1 (imaging condition 1). The left-hand lens must image the center lens back onto itself as the beam is reflected (imaging condition 2 again). Note that the beam passes through the left-hand lens twice.

If the beam entering the lens train arrives on a later bounce, it must pass through CP_1 and progress on to CP_2. Therefore the right-hand lens in lens group (LG) 2, in conjunction with the last lens of the previous lens group, should image the center lens of LG1 onto the center lens of LG2 (second imaging condition). The remaining lenses are chosen in a similar manner.

We next comment on the lens diameters. Note that the magnification from each conjugate plane to any other conjugate plane is $M = -1$. This is because within each lens group the object distance for the center lens is equal to the image distance. This implies that all the lenses adjacent to the conjugate planes have equal diameters that are sufficiently large to cover the spot array. However, the object and image distances for these lenses are not the same, which results in magnification from one center lens to the next. In short, the diameters of the center lenses will tend to increase with increasing lens train length.

Lens Train Design Sample: In this section we present a specific design. We again assume a 16×16 array of 100-μm pixels on a 250-μm pitch on the SLM. We will take the fundamental time increment for the lens train to start at $2^9 = 512$ ps. This example provides 6 total bits of delay in the lens train, ranging from increments between 512 ps and 8,192 ps, for a total maximum delay of 16 ns. The overall length of this lens train is 2.46 m. Our design rules require singlet lenses and f/6 imaging.

Within each lens group, there are right, left, and center lenses with corresponding focal lengths f_c, f_r, and f_l. Table 2 shows the delay time for each lens group, the required focal lengths for each lens within that group, and the required minimum diameters.

Note that the lens on the right-hand side of the first lens group does not have the same focal length as the lens on the left-hand side. This is because the former is positioned at the entrance to the lens train, where there is no corresponding lens to the left-hand side.

Table 2. Specific Values for Lenses in Lens Train Design Sample in Section 3.1

	Lens Group					
Value	1	2	3	4	5	6
Time delay of group (ps)	512	512	1024	2048	4096	8192
f_c (mm)	19.2	19.2	38.4	76.8	253.6	307.2
f_l (mm)	38.4	38.4	76.8	153.6	307.2	614.4
f_r (mm)	30.1	38.4	76.8	153.6	307.2	614.4
D_c (mm)	7.5	7.5	15	30	60	120
D_l (mm)	6.4	6.4	6.4	6.4	6.4	6.4
D_r (mm)	6.4	6.4	6.4	6.4	6.4	6.4

4. Fibers as Delay Elements

Yet another potential solution for producing long delays entails the placement of arrays of fiber in the delay element. One could place a bank of fibers of the same length in each row at the equivalent plane of auxiliary mirror II, with one fiber per input beam and with the length doubling from column to column. One cannot, however, simply put a reflective coating on the backs of the fibers and treat them as individual glass blocks. This is because when the light enters the delay element it arrives from one objective mirror (e.g., mirror E), but when it departs it must go to the other mirror in that White cell, as shown in Fig. 8(a), with the auxiliary mirror standing in for the delay element. (We show the objective mirrors stacked one above the other rather than side by side as in earlier figures; this makes no difference.) When there is a flat mirror, as in Fig. 8(a), light is incident at some angle and reflects at the corresponding angle. In fiber, however, the light must not only have a particular angle with respect to the fiber core, it must also enter and leave at the very same angle, requirements that frustrate White cell operation.

This problem can be avoided, however, by the use of a design such as that shown in Fig. 8(b). Here mirror E images the spots from the SLM onto an array of optical fibers, all tilted to the correct angle. The light propagates through the fibers and emerges at the output plane of the delay element, which is tilted to direct the beams to mirror F. Now mirror F is arranged to image the output faces of those fibers back onto the SLM at the next appropriate spot locations.

The use of fiber may not be practical, however, since on the one hand the fibers must be single mode to avoid modal dispersion that would produce ambiguity in the time delays, whereas on the other hand coupling multiple times into single-mode fiber from free space would be prohibitively lossy. The use of graded index fibers might minimize the intermodal dispersion, but there is debate as to whether the modal coupling would alter the spot size or shape as the beams go through the fibers. In a White cell, the spot that goes into the delay element, whatever it is, should look the same when it comes out, since it will be replicated many times. One can hope that recent developments in the area of photonic band gap fibers with very large single modes will yield a design that simultaneously prevents intermodal dispersion and provides a very large mode for multiple coupling. This is an area for future work.

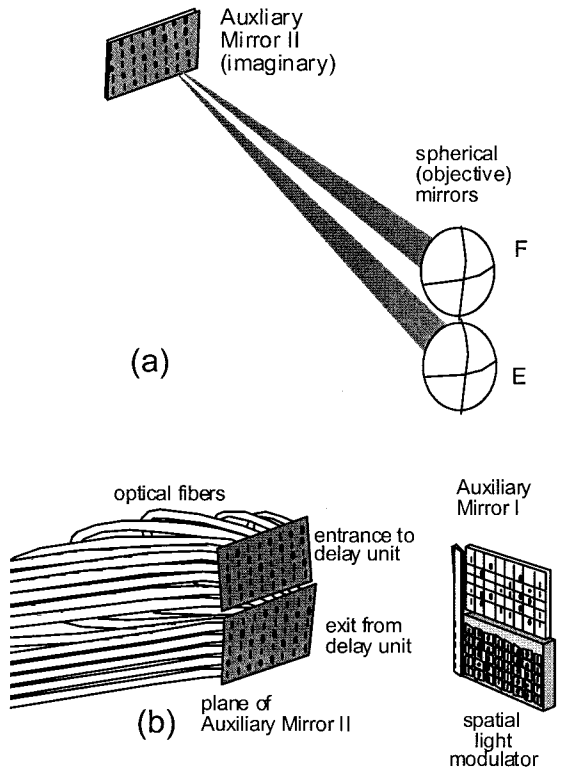

Fig. 8. Fibers as delay elements. The input and output planes are tipped to receive light from mirror E and return it to mirror F. The field lenses are not shown.

5. Loss in Delay Elements

When using optical true-time delay (or any other time-delay device) to steer phased-array antennas, one must keep the loss as low as possible. RF systems are much less forgiving of noise than, say, digital systems. Furthermore it is imperative to keep the losses constant; that is, they should not depend on the delay selected because variations in amplitudes of the signals reaching the antenna elements can cause unintended beam shaping. In this section we analyze the expected losses for delay elements implemented with glass blocks and lens trains as a function of delay selected. We will consider only the losses of the delay elements, not the switching engine (the two White cells and spatial light modulator), for they have been addressed elsewhere[23] in the context of a similar device with the same components. Also discussed in Ref. 23 is interelement cross talk due to imperfect polarization switching stemming from limitations of both the liquid crystal and the beam splitter.

In what follows, we consider reflection and transmission losses in the delay elements. We assume all transmitting surfaces to be treated with antireflective coatings with a loss of 0.25%. We also assume all reflecting surfaces to be dielectric mirrors with reflection coefficients of 0.999. We neglect the effect of truncation losses based on the assumption that, with a precise choice of spot size, the power loss due to truncation by the block edges is less than 0.0001%. Finally, we consider as many as 8 bits of delay in each case.

A. Loss in Glass Blocks

The glass block mechanisms are very simple. The losses that can be expected are Fresnel reflection loss from the front surface of the glass and reflectivity loss from the mirror at the back. The primary assumptions here are that truncation or diffraction losses are negligible and that the fronts of the blocks are antireflection coated. The transmission for a single delay block, neglecting absorption or scattering, is

$$T_{DB} = T_F R_M T_F = R_M T_F^2 = (0.999)(0.9975)^2 = 0.994, \quad (14)$$

or a 0.0218-dB loss.

We can calculate the loss in decibels that occurs in the binary cell with N delay elements (e.g., N glass blocks or N lens groups). If the delay selected is $n\Delta$, then the loss is

$$\text{Loss} = -\{10N \log(T_{SW}) + [f_n(n)]10 \log(R_M) + [N - f_1(n)]10 \log(T_{DB})\}, \quad (15)$$

where R_M is the reflection coefficient of the auxiliary mirror, T_{SW} is the loss per pass through the switching engine, T_{DB} is the transmission through a given delay block, and $f_1(n)$ is the number of times the beam is sent to the null path.

The function $f_1(n)$ is found as follows. First the selected delay (n) is converted to an N-bit binary number. Next we number the bits from least to most significant, letting $i = 1$ represent the least significant bit and $i = 8$ represent the most significant one. We then let a_i be the value of the ith digit (1 or 0) in the binary representation. Then the number of glass blocks visited is equal to $\sum_{i=1}^{N} a_i$, and the number of visits to the null path is given by

$$f_1(n) = N - \sum_{i=1}^{N} a_i. \quad (16)$$

Because the total number of bounces is fixed, N is also fixed and the first term of Eq. (15) is constant. Figure 9 shows the total loss accumulated through the delay blocks, excluding the switching engine, as a function of delay selected. The possible variation in signal strength is ± 0.2 dB.

B. Loss in Lens Train

The loss in the lens train is more complicated. It is given by

$$\text{Loss} = -[10N \log(T_{SW}) + f_1(n)10 \log(R_M) + f_2(n)10 \log(T_L^{2l})]. \quad (17)$$

Here T_L is the transmission of a lens (T_f^2) and l is the number of lenses per lens group (in our case $l = 3$). The procedure for determining the function $f_2(n)$ is as follows. The selected delay (n) is again converted to an N-bit binary number. For example, suppose a delay of 200Δ is selected, and suppose we have an

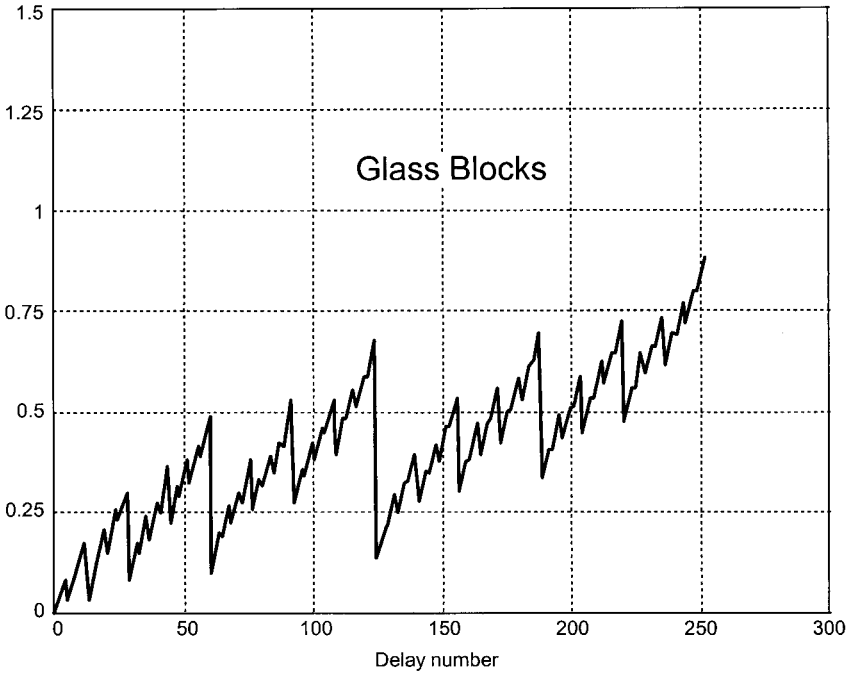

Fig. 9. Losses in the glass block delay element as a function of the delay number.

8-bit system ($N = 8$). The binary representation of 200 is 11001000. On the least significant bit the beam passes through one lens group in the lens train. In our example, however, the least significant bit is zero, so the beam travels the null path instead. On the fourth bit ($i = 4$) our example contains a one, so the beam travels the delay path. Here the beam passes through four lens groups, so the total loss for that pass is four times the loss per lens group. On bit 5, the beam goes to the null path again, and so on. Thus the function $f_2(n)$ represents the total number of lens groups that the beam encounters for a given delay. It is given by

$$f_2(n) = \sum_{i=1}^{N} a_i i. \tag{18}$$

Figure 10 shows the loss in the lens train as a function of delay selected. Note the change in scale compared with Fig. 9 for glass blocks. The total variation in signal power for the lens train is close to 4.7 dB. The loss curve for glass blocks is included for comparison.

In either the glass block or the lens train case, the variation in signal power could be smoothed out by the application of the appropriate attenuation in strips to the auxiliary mirror; that is, the first strip should produce a loss equal to that of the first delay, etc. However, there is no getting around the total loss.

C. Comparison with the Quadratic White Cell Optical True-Time-Delay Device

In previous work we described other, simpler optical true-time-delay devices based on the White cell. In particular, in Ref. 23 we described a quadratic cell with a LC SLM. Like the binary cell, the quadratic cell consists of two White cells joined by a polarizing beam splitter and a SLM. In the binary cell, however, the four spherical mirrors of the White cell are all equidistant from the spot image plane(s). One White cell delivers the spots to a delay device; the other sends the beams to a null path. In the quadratic cell, the spherical mirrors are different distances from the SLM, producing delays that accumulate on every bounce. There is no separate delay-producing device. The number of delays obtainable in a quadratic LC-based true-time-delay White cell is proportional to m^2, as compared with 2^m for the binary cell. The binary function grows much faster, which means that the number of delays it can produce for a given number of bounces will always be better than that produced by the quadratic cell and will have a corresponding lower optical loss.

Figure 11 shows a comparison of the total loss in White-cell–based binary with that in quadratic cells as a function of the maximum possible number of delays. Two binary cells are included: One uses glass blocks as the delay elements and the other uses a lens train with three lenses per group. In all three cases, the losses of the LC SLM and the polarizing beam splitter are included and are all the same. As expected, the losses in the binary cell are much less, and the advantage improves as the number of delays increases. The trade-off is that the binary cell, with its specific delay elements, is more complex and has variation in loss depending on the delay selected. The quadratic cell, on the other hand, has the same loss for all delays because the number of components visited on every pass is the same whether it entails a long White cell arm or a short one.

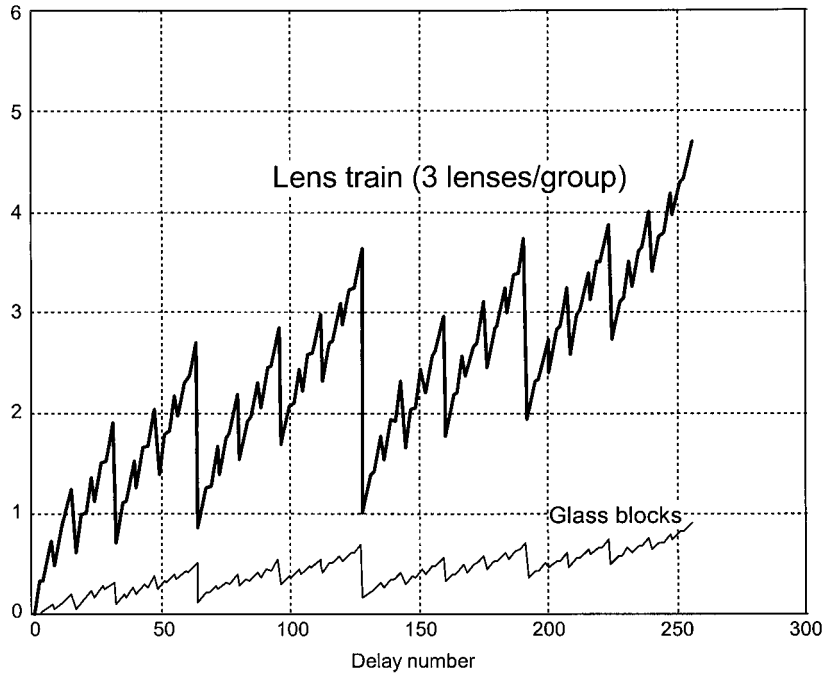

Fig. 10. Loss in the lens train delay elements as a function of the delay selected. This plot assumes three lenses per lens group. The loss for glass block is superimposed for comparison.

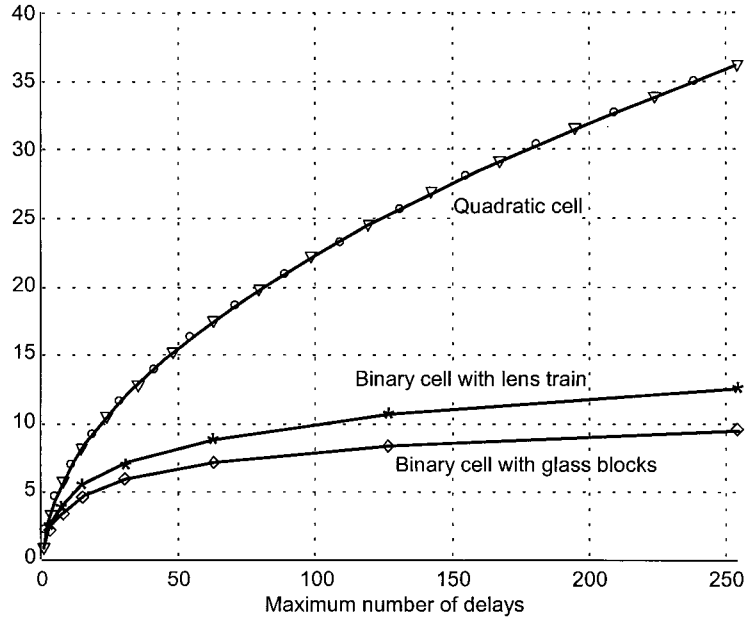

Fig. 11. Loss comparisons among a binary cell with glass blocks, a binary cell with a lens train, and a quadratic cell.[23]

6. Discussion and Summary

From a complexity as well as a loss point of view, the glass blocks offer a delay mechanism in binary White cell–based optical true-time-delay devices that is preferable to the lens trains. The loss for the glass blocks is lower and less variable, which results in better shaping of the radar beams in phased-array antennas. However, because of the inevitable beam divergence associated with glass blocks they are not suitable for long delays. Another solution, such as a lens train, is needed for longer delays.

The reader may have noticed that in our example designs we ended with a maximum delay of 127 ps in the glass block design but started the lens train at 512 ps. The range between requires a little extra effort to achieve. The shortest lens group requires lenses of 19-mm focal length, about as small as can be reasonably achieved with standard singlet lenses of

sufficient diameter to accommodate our postulated SLM. For shorter lens groups, to extend the range to shorter delays will require a more sophisticated lens design to limit the accuracy of aberrations. This is especially important in cases where there are many input beams and the spot array is large.

The range of the glass blocks, on the other hand, can be extended to longer delays by magnifying the SLM plane onto the delay element, by increasing the refractive index of the blocks (e.g., by using lithium niobate or some other high-index material), or by employing some combination of the two.

We have presented two possible delay mechanisms for use in a binary White cell. Compared with earlier quadratic devices the binary cell can produce far more delays for a given number of bounces. Given that optical loss increases with the number of bounces the binary cell offers the distinct advantage of allowing both variables to be minimized.

We mention in passing that liquid crystals may not be optimal for the SLMs. Apart from the issue of environmental robustness, the losses are fairly high, amounting to approximately 1 dB per bounce when the polarizing beam splitter is also taken into account.[23] A microelectromechanical systems (MEMS) tip/tilt mirror array would be preferable. As discussed elsewhere,[27] however, a two-state tip/tilt MEMS mirror, in which the pixels can tip either of two stable states, requires twice as many bounces in a binary cell as with a liquid crystal. On the other hand, MEMS-related losses are expected ultimately to be in the 0.1-dB range, making this an attractive alternative despite the larger number of bounces.

References

1. H. Zmuda and E. N. Toughlian, *Photonic Aspects of Modern Radar*, B. Culshaw, A. Rogers, and H. Taylor, eds. (Artech House, Boston, 1994).
2. W. Ng and A. A. Watson, "The first demonstration of an optically steering microwave phased array antenna using true-time delay," IEEE J. Lightwave Technol. **9,** 1124–1131 (1991).
3. A. P. Goutzoulis and D. K. Davies, "Hardware-compressive 2-D fiber optic delay line architecture for time steering of phased-array antennas," Appl. Opt. **29,** 5353–5359 (1991).
4. P. J. Matthews, M. Y. Frankel, and R. D. Esman, "A wide-band fiber-optic true time-steered array receiver capable of multiple independent simultaneous beams," IEEE Photon. Technol. Lett. **10,** 722–724 (1998).
5. H. Zmuda, E. N. Toughlian, P. Payson, and H. W. Klumpke III, "A photonic implementation of a wide-band nulling system for phased arrays," IEEE Photon. Technol. Lett. **10,** 725–727 (1998).
6. A. P. Goutzoulis, D. K. Davies, and J. M. Zomp, "Hybrid electronic fiber optic wavelength-multiplexed system for true time-steering of phased array antennas," Opt. Eng. **31,** 2312–2322 (1992).
7. A. P. Goutzoulis and J. M. Zomp, "Development and field demonstration of an eight-element receive wavelength-multiplexed true-time-delay steering system," Appl. Opt. **36,** 7315–7326 (1997).
8. R. Taylor and S. Forrest, "Steering of an optical-driven true-time delay phased-array antenna based on a broad-band coherent WDM architecture," IEEE Photon. Technol. Lett. **10,** 144–146 (1998).
9. G. A. Ball, W. H. Glenn, and W. W. Morey, "Programmable fiber optic delay line," IEEE Photon. Technol. Lett. **6,** 741–743 (1994).
10. D. A. Cohern, Y. Chang, G. J. Levi, H. R. Fetterman, and I. L. Newberg, "Optically controlled serially fed phased array sensor," IEEE Photon. Technol. Lett. **8,** 1688–1685 (1996).
11. B. Tsap, Y. Change, H. R. Fetterman, F. J. Levi, D. A. Cohen, and I. Newberg, "Phased array optically controlled receiver using a serial feed," IEEE Photon. Technol. Lett. **10,** 267–269 (1998).
12. J. L. Cruz, L. Dong, S. Barcelso, and L. Reekie, "Fiber Bragg gratings with various chirp profiles in etched tapers," Appl. Opt. **35,** 6781–6787 (1996).
13. M. Tamburrini, M. Parent, L. Goldberg, and D. Stillwell, "Optical feed for a phased array microwave antenna," Electron. Lett. **23,** 680–681 (1987).
14. Z. Fu, C. Zhou, and R. T. Chen, "Waveguide hologram-based wavelength-division multiplexed pseudoanalgo true time-delay module for wide-band phased array antennas," Appl. Opt. **28,** 3053–3059 (1999).
15. R. L. Qi, X. Fu, and R. Chen, "High packing-density 2.5 THz truetime delay lines using spatially multiplexed substrate guided waves in conjunction with volume holograms on a single substrate," J. Lightwave Technol. **15,** 2253–2258 (1997).
16. L. Eldada, "Laser-fabricated delay lines in GaAs for optically steered phased-array radar," J. Lightwave Technol. **13,** 2034–2039 (1995).
17. X. S. Yao and L. Maleki, "A novel 2-D programmable photonic time-delay device for millimeter wave signal processing applications," IEEE Photon. Technol. Lett. **6,** 1463–1465 (1994).
18. M. Madamopoulos and N. Riza, "Directly modulated semiconductor-laser-fed photonic delay line with ferroelectric liquid crystals," Appl. Opt. **27,** 1407–1416 (1998).
19. N. A. Riza, "25-Channel nematic liquid-crystal optical time-delay unit characterization," IEEE Photon. Technol. Lett. **7,** 1285–1287 (1995).
20. E. N. Toughlian and H. Zmuda, "A photonic variable RF delay line for phased array antennas," J. Lightwave Technol. **8,** 1824–1828 (1990).
21. S. A. Collins, Jr. and B. L. Anderson, "Device and method for producing optically-controlled incremental time delays," U.S. patent 6,388,615 (14 May 2002).
22. B. L. Anderson and R. Mital, "Polynomial-based optical true-time delay devices using MEMS," Appl. Opt. **41,** 5449–5461 (2002).
23. B. L. Anderson and C. D. Liddle, "Optical true-time delay for phased array antennas demonstration of a quadratic White cell," Appl. Opt. **41,** 4912–4921 (2002).
24. J. White, "Long paths of large aperture," J. Opt. Soc. Am. **32,** 285–288 (1942).
25. R. Higgins, N. K. Nahar, and B. L. Anderson, "Design and demonstration of a switching engine for a binary true-time-delay device that uses a White cell," Appl. Opt. **42,** 4747–4757 (2003).
26. B. L. Anderson, S. A. Collins, Jr., C. A. Klein, E. A. Beecher, and S. B. Brown, "Photonically produced true-time delays for phased antenna arrays," Appl. Opt. **36,** 8493–9503 (1997).
27. V. Argueta-Diaz and B. L. Anderson, "Reconfigurable photonic switch based on a binary system using the White cell and micromirror arrays," J. Special Topics in Quantum Electron. (to be published).